TWO SCALE HOMOGENIZATION IN TERNARY LOCALLY RESONANT METAMATERIALS

C. Comi[1*], M. Moscatelli[1,2], J-J. Marigo[2]

[1] Dept. of Civil and Environmental Eng. - Politecnico di Milano, P.za L. da Vinci 32, 20133 Milano, Italy

[2] Laboratoire de Mécanique des Solides, Ecole polytechnique, Palaiseau, France

* claudia.comi@polimi.it

Abstract.
In this work, we exploit the two-scale homogenization approach to compute explicitly the band gaps for out-of-plane wave propagation in ternary locally resonant metamaterials (LRM) with two-dimensional periodicity. The homogenization approach, recently developed by the authors for binary LRM, leads to the definition of the dynamic effective mass density, depending on the frequency, that becomes negative near the resonant frequencies of the inclusions. The intervals of negative effective mass give the band gaps. These explicit solutions put in evidence the dependence of the spectral gaps on the geometric parameters of the unit cell and on the mechanical properties of the three constituent materials. The range of frequency where the asymptotic homogenization approach is equivalent to the Bloch-Floquet theory is also established and confirmed by numerical simulations.

1. Introduction

Sonic and phononic crystals based on the localized resonant principle have been proposed and studied in the last twenty years. In particular, periodic materials with heavy, stiff inclusions with a soft coating embedded in a stiff matrix have been demonstrated to have broad spectral gaps at low frequency, see e.g. [1] with pioneering experimental results on a composite with lead spheres coated by silicone rubber in epoxy matrix. The intervals of frequency inside which no waves with real wavenumber can propagate, can have different applications especially in vibration isolation [2],[3] or impact absorption [4],[5].

The physical mechanism of local resonance with the corresponding spectral gaps can be associated with the concept of negative effective mass. This can be well understood with help of simple discrete mass-spring structures and many works have been performed in this direction, see e.g.[6] [7]. Also in actual continuum composites one can, by different approaches, define an equivalent, effective mass density. In particular in [8] and [9] quite complex expressions of the effective mass were derived for ternary composites considering a single cell with rigid cylindrical or spherical inclusions coated by a soft materials and the possibility of negative effective mass were demonstrated. However, the limit of validity of these solutions was not explicitly settled.

The two-scale homogenization approach, first proposed in [10] for high-contrast binary elastic composite materials in the long wavelength regime, provides a powerful tool to define equivalent material properties. In [11] the approach was developed for a row of locally resonant inclusions and recently the authors studied the spectral properties and the band gaps of binary LRM through homogenization, [12].

In the same line, in the present work, we address the problem of out-of-plane wave propagation in ternary LRM by the two-scale homogenization approach. The material has two-dimensional periodicity, with cylindrical inclusions, modelled as rigid, coated by a very compliant material. In the low frequency regime, under the hypothesis of high contrast between the stiffness of the coating and of the matrix, homogenization leads to the definition of the dynamic effective mass density, depending on the frequency, that becomes negative near the resonant frequencies of the inclusions. The intervals of negative effective mass give the band

gaps. The influence of geometric parameters of the unit cell, such as the filling fraction or the coating thickness, on the spectral gaps can thus be simply studied. This can be useful for the design of the metamaterial.

The paper is organized as follows. Section 2 sets the problem and the basic assumptions. The homogenization approach is developed in Section 3, where a closed form expression for the effective mass is derived. Results in terms of band gaps for different LRM are shown in Section 4. Section 5 provides a comparison of the analytical results with the numerical results obtained on a single cell with Bloch-Floquet boundary conditions; the range of frequency where the asymptotic homogenization approach is equivalent to the Bloch-Floquet theory is also established and confirmed by the simulations. Some conclusions are given in Section 6.

2. Problem formulation

We consider out-of-plane wave propagation in a ternary material endowed with two dimensional periodicity. The heterogeneous body Ω has a cross section S in the plane x_1-x_2 and has a length in the direction x_3 very large with respect to the heterogeneities, see Fig. 1a. The unit cell that periodically repeats in the plane x_1-x_2 is composed by a stiff matrix m containing a cylindrical heavy inclusion (also referred to as fibers, f) coated by a very compliant material c, as shown in Fig. 1b. The matrix and the coating are isotropic with linear elastic behavior, while the fiber is considered as rigid. The two dimensional Bravais lattice has primitive vectors $\mathbf{a}_1$ and $\mathbf{a}_2$, which can have different moduli and can be non-orthogonal.

In this work, we assume that the size $a = \|\mathbf{a}_1 \wedge \mathbf{a}_2\|$ of the in-plane area Y^ϵ of the unit cell is small with respect to the considered wavelengths in the matrix material L_m

$$a = \epsilon L_m = \frac{\epsilon}{\omega}\sqrt{\frac{\mu_m}{\rho_m}} \tag{1}$$

with ϵ a dimensionless small parameter, ω the angular frequency of the wave, μ_m the elastic shear modulus and ρ_m the mass density of the matrix. The coated inclusion has radius $R_c^\epsilon = \epsilon R_c$ and the heavy stiff core has radius $R_f^\epsilon = \epsilon R_f$. The area of the coating and of the fiber inside the unit cell are Y_c^ϵ and Y_f^ϵ, respectively. The filling fraction ϕ is defined as the ratio between the area of the coated inclusion and the total area

$$\phi = \frac{|Y_f^\epsilon| + |Y_c^\epsilon|}{|Y^\epsilon|} \tag{2}$$

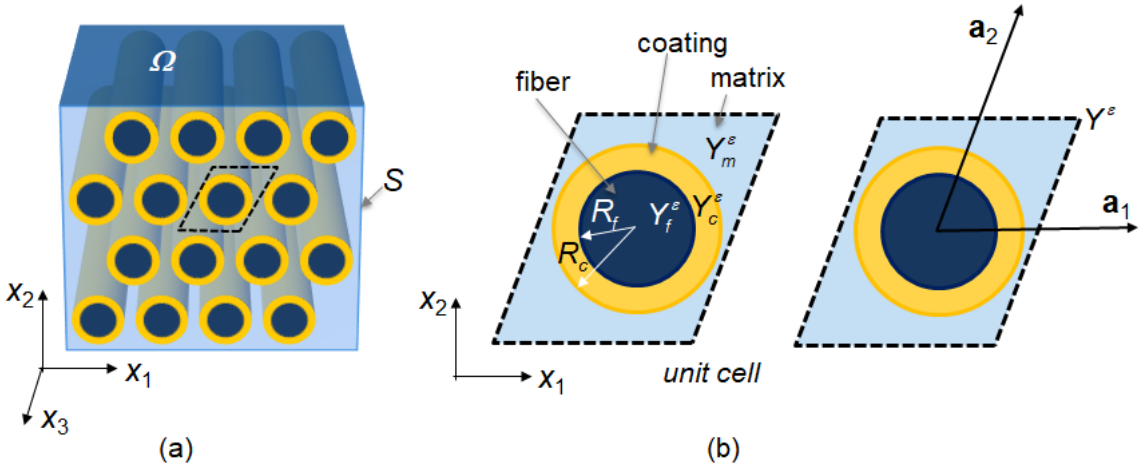

Figure 1. Metamaterial with periodically distributed coated cylindrical inclusions: (a) geometry, (b) unit cell with primitive vectors $\mathbf{a}_i$.

We further assume that there is high contrast between the stiffness of the matrix and that of the coating, namely the ratio between the elastic shear modulus of the coating and of the matrix is of the order of ϵ^2. We denote by $\epsilon^2\mu_c$ the coating shear modulus, with μ_c of the order of μ_m, and by ρ_c its mass density.

The motion, for a wave of angular frequency ω with out-of-plane polarization, is described by a displacement field, which has only one component $u^\epsilon = u_3^\epsilon$ in the direction x_3 that depends only on the in-plane coordinates x_1 and x_2. The non-vanishing stress components σ_{31}^ϵ and σ_{32}^ϵ are collected in vector $\boldsymbol{\sigma}^\epsilon$ that reads:

$$\boldsymbol{\sigma}^\epsilon = \mu^\epsilon \operatorname{grad} u^\epsilon \text{ in } \Omega, \tag{3}$$

with μ^ϵ equal to $\epsilon^2\mu_c$ in Y_c^ϵ and μ_m in Y_m^ϵ. In view of the simplifying assumption of rigid inclusion, the stress in Y_f^ϵ is only fixed by equilibrium.

The equation of motion is expressed by:

$$\operatorname{div} \boldsymbol{\sigma}^\epsilon + \rho^\epsilon \omega^2 u^\epsilon = 0 \text{ in } \Omega \tag{4}$$

The two scale asymptotic method [13], [11] allows to construct the homogenized equation of motion for the composite material and to derive analytical conditions for wave propagation and band gaps prediction.

3. Homogenization approach

Let us introduce first the rescaled unit cell $Y = Y^\epsilon/\epsilon$ and a microscopic coordinate $\mathbf{y}=\mathbf{x}/\epsilon$ within it. The displacement and the stress are expanded in the form:

$$u^\epsilon(\mathbf{x}) = u^0(\mathbf{x}, \mathbf{x}/\epsilon) + \epsilon u^1(\mathbf{x}, \mathbf{x}/\epsilon) + \epsilon^2 u^2(\mathbf{x}, \mathbf{x}/\epsilon) + \dots \tag{5}$$

$$\boldsymbol{\sigma}^\epsilon(\mathbf{x}) = \boldsymbol{\sigma}^0(\mathbf{x}, \mathbf{x}/\epsilon) + \epsilon \boldsymbol{\sigma}^1(\mathbf{x}, \mathbf{x}/\epsilon) + \epsilon^2 \boldsymbol{\sigma}^2(\mathbf{x}, \mathbf{x}/\epsilon) + \dots \tag{6}$$

The fields $u^\alpha = u^\alpha(\mathbf{x}, \mathbf{y})$ and $\boldsymbol{\sigma}^\alpha = \boldsymbol{\sigma}^\alpha(\mathbf{x}, \mathbf{y})$, $\alpha = 0, 1, 2, \dots$, depend of both the macroscopic $\mathbf{x}$ and microscopic $\mathbf{y}$ coordinates and are Y-periodic with respect to $\mathbf{y}$. Accordingly, their spatial partial derivatives are denoted by an index $\mathbf{x}$ or $\mathbf{y}$. From (5) and (6) one obtains:

$$\operatorname{grad} u^\epsilon(\mathbf{x}) = \epsilon^{-1}\operatorname{grad}_\mathbf{y} u^0 + \operatorname{grad}_\mathbf{y} u^1 + \operatorname{grad}_\mathbf{x} u^0 + \epsilon(\operatorname{grad}_\mathbf{y} u^2 + \operatorname{grad}_\mathbf{x} u^1) + \dots \tag{7}$$

$$\operatorname{div} \boldsymbol{\sigma}^\epsilon(\mathbf{x}) = \epsilon^{-1} \operatorname{div}_\mathbf{y} \boldsymbol{\sigma}^0 + \operatorname{div}_\mathbf{y} \boldsymbol{\sigma}^1 + \operatorname{div}_\mathbf{x} \boldsymbol{\sigma}^0 + \epsilon(\operatorname{div}_\mathbf{y} \boldsymbol{\sigma}^2 + \operatorname{div}_\mathbf{x} \boldsymbol{\sigma}^1) + \dots \tag{8}$$

The expansions (5-8) are substituted in the governing equations (3-4) and the terms of the same order in ϵ are then considered.

At order -1 from (3) we get $\operatorname{grad}_\mathbf{y} u^0 = 0$ in Y_m and Y_f, while from (4) we get $\operatorname{div}_\mathbf{y} \boldsymbol{\sigma}^0 = \mathbf{0}$ in Y. Hence:

$$u^0(\mathbf{x}, \mathbf{y}) = U_m^0(\mathbf{x}) \text{ in } S \times Y_m; \quad u^0(\mathbf{x}, \mathbf{y}) = U_f^0(\mathbf{x}) \text{ in } S \times Y_f \tag{9}$$

and

$$\boldsymbol{\sigma}^0 = \mu_m(\operatorname{grad}_\mathbf{x} U_m^0 + \operatorname{grad}_\mathbf{y} u^1) \text{ in } S \times Y_m; \quad \boldsymbol{\sigma}^0 = \mathbf{0} \text{ in } S \times Y_c \tag{10}$$

The term $\operatorname{grad}_\mathbf{x} U_m^0$ in eq. (10) can be interpreted as a constant eigenstrain in the cell. For any value of $\operatorname{grad}_\mathbf{x} U_m^0$, one can solve a linear elastic static problem in the matrix only, with periodic boundary conditions, subject to the additional condition of zero stress at the boundary with the coating ∂Y_c. The out-of-plane displacement u^1 in the matrix can be expressed as

$$u^1(\mathbf{x}, \mathbf{y}) = \sum_{i=1}^{2} \frac{\partial U_m^0}{\partial x_i}(\mathbf{x}) \chi^i(\mathbf{y}) + U^1(\mathbf{x}) \text{ in } S \times Y_m \tag{11}$$

with χ^i solution of the problem

$$\begin{cases} \operatorname{div} \operatorname{grad}_\mathbf{y} \chi^i = 0 & \text{in } Y_m \\ \mu_m(\operatorname{grad}_\mathbf{y} \chi^i + \mathbf{e}_i) \cdot \mathbf{n} = 0 & \text{on } \partial Y_c \\ \chi^i \text{ periodic}, \ \mu_m \operatorname{grad}_\mathbf{y} \chi^i \cdot \mathbf{n} \text{ anti-periodic} & \text{on } \partial Y \end{cases} \tag{12}$$

$\mathbf{e}_i$ being the unit vector of the axis x_i.
The stress in the matrix reads

$$\boldsymbol{\sigma}^0(\mathbf{x},\mathbf{y}) = \sum_{i=1}^{2} \mu_m (\mathrm{grad}_{\mathbf{y}} \chi^i + \mathbf{e}_i) \frac{\partial U_m^0}{\partial x_i}(\mathbf{x}) \text{ in } S \times Y_m \tag{13}$$

The homogenized displacement u^0 in the coating is the solution of the following problem, obtained by considering the terms of order 0 in ϵ in equilibrium equation (4) and those of order 1 in ϵ in the constitutive equation (3):

$$\begin{cases} \mu_c \mathrm{div}\,\mathrm{grad}_{\mathbf{y}} u^0 + \rho_c \omega^2 u^0 = 0 & \text{in } S \times Y_c \\ u^0 = U_m^0 & \text{on } S \times \partial Y_c \\ u^0 = U_f^0 & \text{on } S \times \partial Y_f \end{cases} \tag{14}$$

For a given U_m^0 and a given ω, different from the eigen-frequencies of the coated inclusion fixed at its boundary ∂Y_c, problem (14) admits a unique solution that can be expressed as:

$$u^0(\mathbf{x},\mathbf{y}) = U_m^0(\mathbf{x}) \eta(\mathbf{y}) \text{ in } S \times Y_c \tag{15}$$

where $\eta(\mathbf{y})$ is the solution of

$$\begin{cases} \mathrm{div}\,\mathrm{grad}_{\mathbf{y}} \eta + k^2 \eta = 0 & \text{in } Y_c \\ \eta = 1 & \text{on } \partial Y_c \\ \eta = U_f^0 / U_m^0 & \text{on } \partial Y_f \end{cases} \tag{16}$$

with: $k = \omega \sqrt{\dfrac{\rho_c}{\mu_c}}$.

The displacement of the rigid fiber U_f^0 is obtained from the global dynamic equilibrium of the fiber subject to inertia forces and surface tractions transmitted by the coating

$$\rho_f |Y_f| \omega^2 U_f^0 + \int_{\partial Y_f} \mu_c \, \mathrm{grad}_{\mathbf{y}} \eta(\mathbf{y}) \cdot \mathbf{n} \, d\mathbf{y} \, U_m^0 = 0 \tag{17}$$

For the coated circular inclusion, problem (16)-(17) can be solved in close form and the solution in polar coordinates ($r = \|\mathbf{y}\|$) for $R_f \le r \le R_c$ reads:

$$\eta(\mathbf{y}) = \frac{kR_f \rho_f \left(J_0(kr) Y_0(kR_f) - Y_0(kr) J_0(kR_f) \right) + 2\rho_c \left(Y_0(kr) J_1(kR_f) - J_0(kr) Y_1(kR_f) \right)}{den} \tag{18}$$

with

$$den = kR_f \rho_f \left(J_0(kR_c) Y_0(kR_f) - Y_0(kR_c) J_0(kR_f) \right) + 2\rho_c \left(Y_0(kR_c) J_1(kR_f) - J_0(kR_c) Y_1(kR_f) \right) \tag{19}$$

where J_0 and J_1 are Bessel function of the first kind and Y_0 and Y_1 are Bessel function of the second kind.

The ratio between the displacement in the fiber and in the matrix reads

$$\frac{U_f^0}{U_m^0} = \eta(R_f) = \frac{2\rho_c \left(Y_0(kR_f) J_1(kR_f) - J_0(kR_f) Y_1(kR_f) \right)}{den} \tag{20}$$

The discussion for ω equal to an eigenfrequency of the coated inclusion follows the same lines of the case of binary metamaterials developed in [12] and is not reported here for brevity.

Having obtained the above solutions for u^0 and $\boldsymbol{\sigma}^0$ in the three constituent matrials one can finally obtain an effective equation of motion for the propagation of out-of-plane waves in the metamaterial. To this purpose, let us consider the expansion of the equation of motion at order 0:

$$\mathrm{div}_{\mathbf{y}} \boldsymbol{\sigma}^1 + \mathrm{div}_{\mathbf{x}} \boldsymbol{\sigma}^0 + \rho \omega^2 u^0 = 0 \quad \text{in } S \times Y \tag{21}$$

and let us integrate it over Y. The integral of the first term equals the integral on the cell boundary of the traction forces which vanishes by virtue of the periodic boundary conditions. The other two terms give

$$\mathrm{div}_{\mathbf{x}}(\mathbf{M}^{*}\mathrm{grad}_{\mathbf{x}}U_m^0)+\rho^{*}(\omega)\,\omega^2\,U_m^0=0 \quad \text{in } S \tag{22}$$

where $\mathbf{M}^{*}$ is the second order effective stiffness tensor, whose components are given by

$$M_{ij}^{*}=\frac{1}{|Y|}\int_{Y_m}\mu_m(\mathrm{grad}_{\mathbf{y}}\chi^i+\mathbf{e}_i)\cdot(\mathrm{grad}_{\mathbf{y}}\chi^j+\mathbf{e}_j)\,d\mathbf{y}, \tag{23}$$

and $\rho^{*}(\omega)$ is the effective mass density. This latter reads

$$\rho^{*}(\omega)=\rho_m\frac{|Y_m|}{|Y|}+\rho_f\frac{|Y_f|}{|Y|}\frac{U_f^0}{U_m^0}+\frac{\rho_c}{|Y|}\int_{Y_c}\eta(\mathbf{y})\,d\mathbf{y}. \tag{24}$$

Using the expression (18) of η one has

$$\int_{Y_c}\eta(\mathbf{y})\,d\mathbf{y}=2\pi(h(R_c)-h(R_f)) \tag{25}$$

with

$$h(r)=\frac{r}{k}\frac{kR_f\rho_f\left(J_1(kr)Y_0(kR_f)-Y_1(kr)J_0(kR_f)\right)+2\rho_c\left(Y_1(kr)J_1(kR_f)-J_1(kr)Y_1(kR_f)\right)}{den} \tag{26}$$

which, inserted into (24) together with (20), gives the explicit form of the effective mass. For ω=0 the integral in (25) is $|Y_c|$, and $U_f^0=U_m^0$, hence the effective mass coincides with the static mass density of the composite material ρ_{st}:

$$\rho_{st}=\rho_m\frac{|Y_m|}{|Y|}+\rho_f\frac{|Y_f|}{|Y|}+\rho_c\frac{|Y_c|}{|Y|} \tag{27}$$

The effective mass is not defined for the frequencies ω_n which are roots of *den*=0 (eq. 19), it tends to -∞ and +∞ when ω tends to ω_n from above and from below, respectively. Therefore, the effective mass density is negative in a countable set of intervals. The values of ω_n, which fix the position of these intervals, depend only on the geometry and material properties of the coating through the non-dimensional groups kR_f and kR_c defined for the rescaled problem in Y. The corresponding real physical quantities in Y^{ϵ} are defined as

$$k^{\epsilon}=\omega\sqrt{\frac{\rho_c}{\epsilon^2\mu_c}}\ ,\ R_f^{\epsilon}=\epsilon R_f\ ,\ R_c^{\epsilon}=\epsilon R_c\ , \tag{28}$$

hence $k^{\epsilon}R_f^{\epsilon}=kR_f$ and $k^{\epsilon}R_c^{\epsilon}=kR_c$ and the frequencies intervals determined with the above analysis remain valid for the physical problem.

In view of eq. (22), waves with frequency ω such that the effective mass density becomes negative cannot propagate inside the composite material; the interval of negative effective mass identify then the band gaps. One should remark however that the homogenization approach applies only to waves with low frequency, as specified by hypothesis (1). This condition involves the properties of the matrix material and should be checked for the particular cases considered.

4. Results

Figure 2a shows the variation of the effective mass density, normalized with the static one, with the frequency $\omega/2\pi$ for the ternary metamaterial constituted by lead inclusions coated with rubber and embedded in epoxy matrix. The ratio between the external radius and internal radius of the coating is 0.2, the filling fraction is $\phi=\pi R_c^2/|Y|=0.4$ and the materials parameters are listed in Table 1. The effective mass becomes negative in several intervals of frequency (shaded in the figure) that correspond to band gaps.

The influence of the thickness of the coating is highlighted in Fig. 2b, where the regions of negative effective mass are shown at varying R_f/R_c. The dashed line corresponds to the effective mass evolution shown in Fig. 2a. The amplitude of the first band gap increases as the

thickness of the coating decreases since, at fixed filling ratio, this corresponds to an increase of the resonating fiber mass.

Table 1. Materials properties.

Constituents	E [MPa]	ν [-]	ρ [Kg/m3]
matrix – epoxy	3600.	0.370	1180.
coating – rubber	0.118	0.469	1300.
inclusion – lead	14000.	0.420	11340.

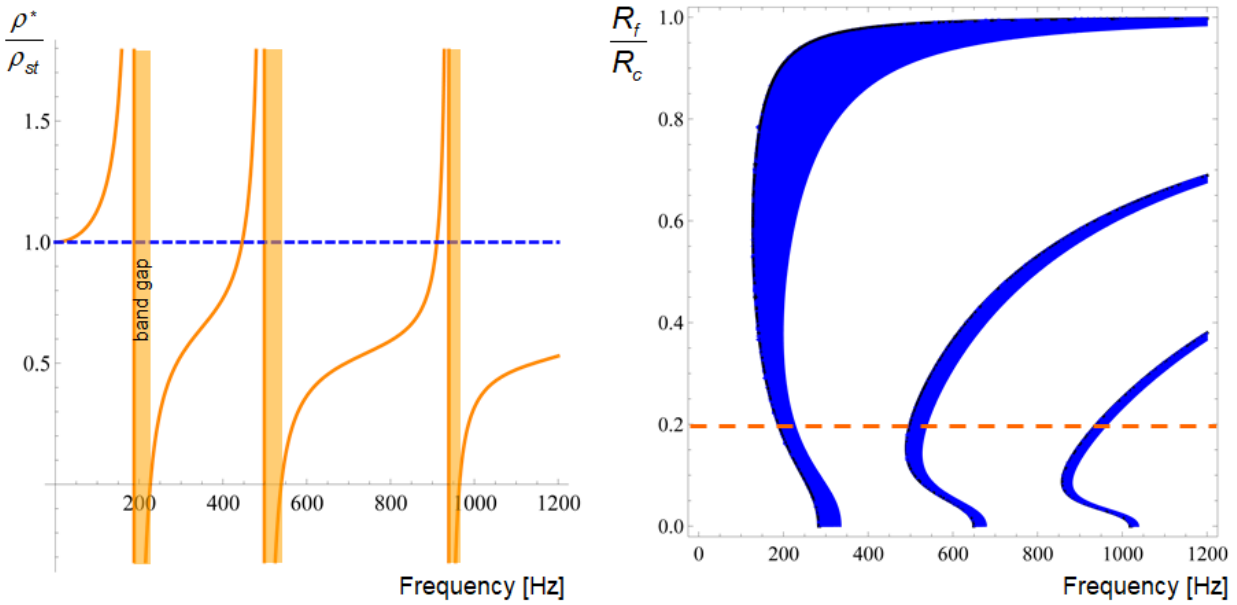

Figure 2. Ternary metamaterial with filling fraction 0.4: (a) normalized effective mass vs. frequency for $R_f / R_c = 0.2$, intervals of negative effective mass give the first three band gaps; (b) intervals of negative effective mass in the plane frequency- R_f / R_c, the dashed line corresponds to the case shown on the left.

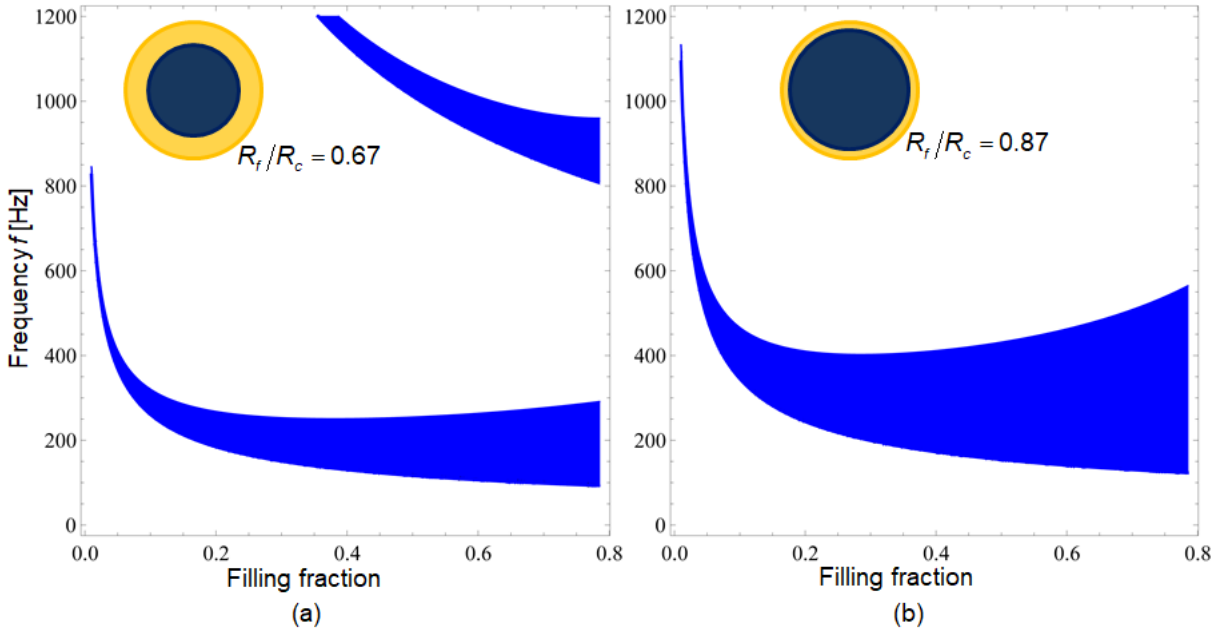

Figure 3. Frequency intervals of negative effective mass for varying filling fraction: (a) thick coating $R_f / R_c = 0.67$, (b) thin coating $R_f / R_c = 0.87$.

Since a closed form solution is obtained, one can easily perform parametric studies to evidence the influence of different geometries on the wave propagation properties.

As an example, Fig. 3 displays the frequency intervals of negative effective mass at varying fillings fractions for the case of a thick coating (Fig. 3a) and that of a thin coating (Fig.3b).

In the first case, two strips are visible since two band gaps are inside the considered interval of frequency, while for the thin coating only the first band gap is inside the considered interval. In both cases, as the filling fraction increases, the opening frequency of the first band gap decreases and the amplitude of the bandgap increases.

5. Discussion and comparison with Bloch-Floquet analysis

The propagation of waves in periodic materials is often studied making use of the Bloch-Floquet theory solving an eigen-problem for the elementary cell subject to peculiar boundary conditions. These latter, also called Bloch-Floquet boundary conditions, relate the displacements of opposite sides of the unit cell and depend on the wave vector **k** considered. The dispersion surfaces, $\omega=\omega(\mathbf{k})$ can be numerically evaluated, e.g. by finite elements [14], [15].

Due to the periodicity and to the symmetries of the unit cell (if any), the description of the dynamic behavior of the metamaterial for all the possible wave vectors can be obtained by considering only the first Irreducible Brillouin Zone (IBZ) of the reciprocal lattice. Furthermore, often only the wave vectors along the boundary of the IBZ are considered, see [16], [17] for details. The frequency of each mode is then plotted as a function of the arc length along the boundary of the IBZ. The diagrams thus obtained are called dispersion diagrams and characterize the transmission properties of the periodic material. The intervals of frequencies where no real solutions exist define the band-gaps.

In a recent work [12], the authors proved that the asymptotic analysis of the Bloch-Floquet problem leads to the same effective equation of motion (20) obtained through the two scale homogenization methods described is Section 3. The two approaches therefore, in the low frequency range, give the same prediction of the band structure. In the following we illustrate these results for the ternary material with two dimensional periodicity.

We refer to the material shown in Fig.1. To perform the numerical analysis, we consider that the inclusions are distributed on S following a square lattice, characterized by orthogonal base vectors $\mathbf{a}_1$ and $\mathbf{a}_2$ with the same modulus, so that the unit cell is a square of side a.

Note that the results of the homogenization theory are general, independent from the actual shape of the unit cell, while of course the numerical analysis of the Bloch-Floquet problem requires to fix the shape of the unit cell.

Assuming a square primary lattice, the reciprocal lattice of wave vectors is also square and the Brillouin Zone is a square with side $2\pi/a$. Exploiting symmetries, the IBZ is the triangle Γ–X–M, shown in the inset of Fig. 4a. The properties of the constituent materials are reported in Table 1.

Figure 4a shows the dispersion plot for the metamaterial with a = 21mm, R_c = 7.5 mm, (corresponding to filling fraction of 0.4) and R_f = 5 mm. The band gaps are shaded and the relative amplitude, defined as the bandwidth divided by the central band-gap frequency, is also reported. Figure 4b shows the evolution of the normalized effective mass density with frequency obtained through homogenization (note that this diagram in rotated of $\pi/2$ to facilitate the comparison). The shaded regions correspond to negative effective mass density and hence give the homogenization-based predictions of band gaps. One can observe an extremely good agreement of the two approaches for the determination of the first band gap.

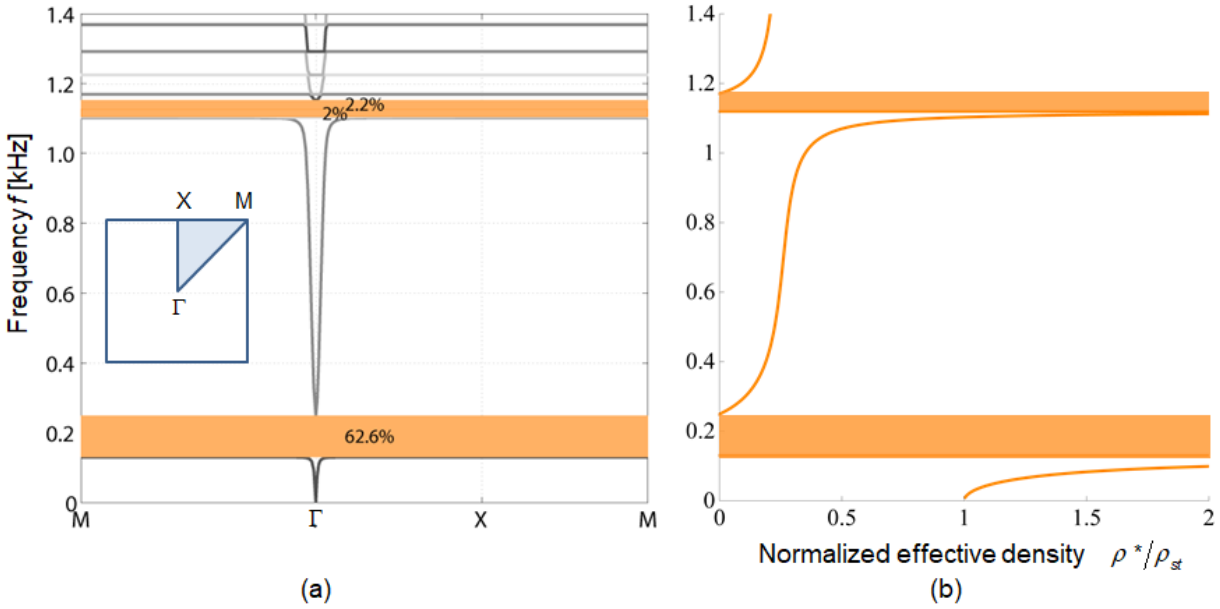

Figure 4. Three components metamaterial, filling fraction 0.4, $R_f / R_c = 0.67$: (a) dispersion plot with dashed bandgaps, (b) normalized effective mass density vs frequency, shaded areas correspond to negative effective mass.

The opening and the closing modes of the first band gap are shown in Fig. 5a-b, they are axial symmetric and correspond to different symmetry points of the IBZ, as common for band-gaps generated by a local resonant mechanism. The second band gap in the dispersion plot is actually separated into two smaller bandgaps by the flat modes shown in figure 5d, and 5e corresponding to local resonances inside the coating characterized by displacement depending on both the radial and the angular coordinates.

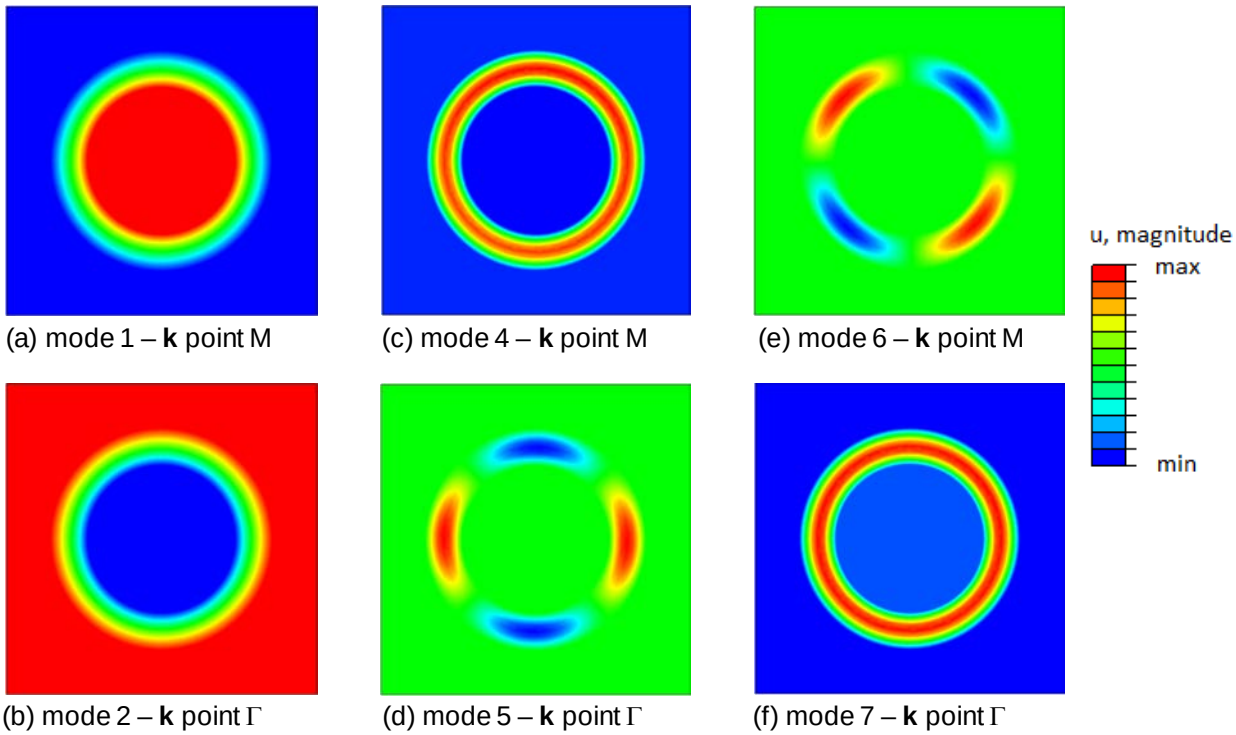

Figure 5. Three components metamaterial, filling fraction 0.4, $R_f / R_c = 0.67$: (a) opening mode of first band gap, (b) closing mode of first band gap, (c) opening mode of second band gap, (d-e) flat modes inside second band gap, (f) closing mode of second band gap.

The prediction of these flat modes through the homogenization approach would require to consider more general, not axial-symmetric, solutions. This part is not developed in this paper. The opening mode of the first part of this second band gap, shown in Fig. 5c, and the closing mode of the second part of this second band gap, Fig 5f, are again axial-symmetric. From Fig. 5 one can also observe that the displacement is uniform in the internal lead inclusion, the hypothesis of rigid inclusion is therefore justified.

Another comparison between the two approaches is presented in Fig. 6 for the metamaterial with inclusions with a thin coating (R_c = 7.5 mm and R_f = 6.5 mm). The agreement is very good also in this case, especially as far as the first band gap is concerned.

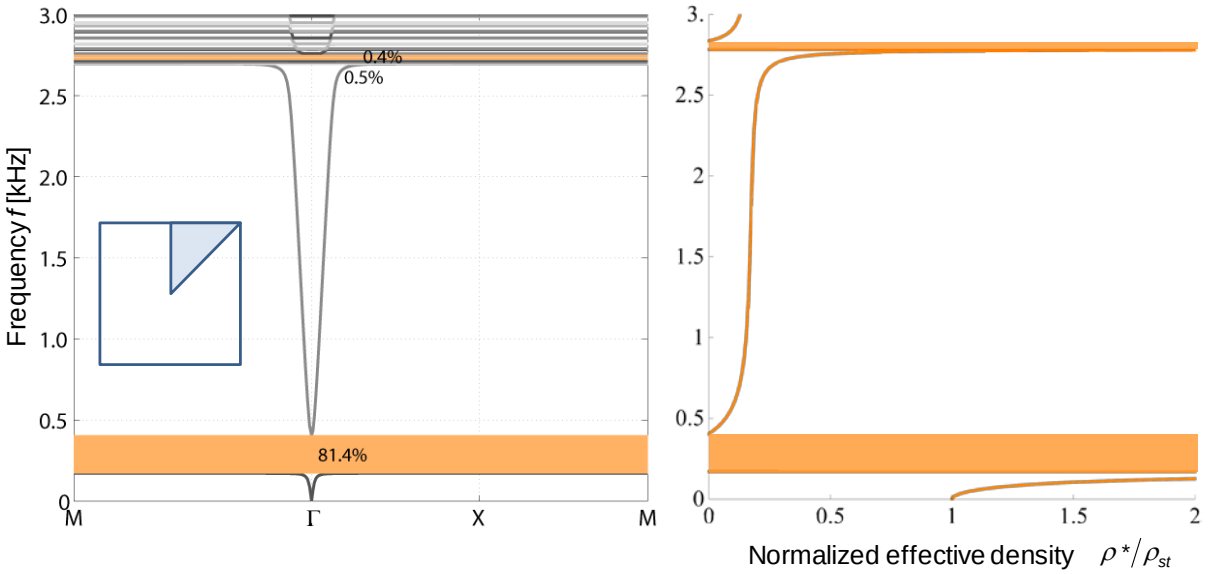

Figure 6. Three components metamaterial, filling fraction 0.4, R_f / R_c = 0.87: (a) dispersion plot with dashed bandgaps, (b) normalized effective mass density vs frequency, shaded areas correspond to negative effective mass.

One should remark that, in both cases considered in Figs. 4 and 6, the first band gaps fall inside the domain of validity of the homogenization approach, which is based on hypothesis (1). In fact, using the properties of the epoxy matrix and the cell dimension a, from (1) one obtains the following limit of validity of the asymptotic analysis: $f << \quad f_{\max} = \frac{1}{2\pi a}\sqrt{\frac{\mu_m}{\rho_m}} = 8\,\text{kHz}$; the frequency of the actual first band gaps are one order of magnitude lower than $f_{\max}$.

6. Conclusions

Based on the two-scale homogenization approach, we present an analytical expression for the dynamic effective mass density of a ternary LRM with cylindrical inclusions. The results, which provide an estimate of the band gaps in the low frequency regime, are independent from the shape of the unit cell and from the matrix stiffness. On the contrary, the gaps in the spectral properties strongly depends on the filling fraction and on the thickness and stiffness of the coating. This dependence is explicitly given in this work.

The range of validity of the homogenization approach is given and the results are also validated by comparison with those numerically obtained from the Bloch-Floquet theory.

The findings may be useful in designing LRM for specific applications where the required band gap frequencies are fixed. The extensions to in-plane wave propagation and spherical inclusions do not bring conceptual difficulties and are currently under development.

Acknowledgements - Financial support of the Italian MIUR (PRIN project nr.2015LYYXA8 on Multi-scale mechanical models for the design and optimization of micro-structured smart materials and metamaterials) and of the Laboratoire de Mécanique des Solides are gratefully acknowledged.

References

[1] Z. Liu, Z. Liu, X. Zhang, Y. Mao, and Y. Y. Zhu, "Locally Resonant Sonic Materials," *Science (80-.).*, vol. 289, no. September, pp. 1734–1736, 2000.

[2] K. T. Tan, H. H. Huang, and C. T. Sun, "Blast-wave impact mitigation using negative effective mass density concept of elastic metamaterials," *Int. J. Impact Eng.*, vol. 64, pp. 20–29, 2014.

[3] L. D'Alessandro *et al.*, "Modelling and experimental verification of a single phase three-dimensional lightweight locally resonant elastic metamaterial with complete low frequency bandgap," in *11th International Congress on Engineered Material Platforms for Novel Wave Phenomena, Metamaterials 2017*, 2017, pp. 70–77.

[4] D. Briccola, M. Ortiz, and A. Pandolfi, "Experimental Validation of Metaconcrete Blast Mitigation Properties," *J. Appl. Mech.*, vol. 84, no. 3, p. 031001, 2016.

[5] C. Comi and L. Driemeier, "Metamaterials for crashworthiness of small cars," in *AIMETA 2017 - Proceedings of the 23rd Conference of the Italian Association of Theoretical and Applied Mechanics*.

[6] H. H. Huang, C. T. Sun, and G. L. Huang, "On the negative effective mass density in acoustic metamaterials," *Int. J. Eng. Sci.*, vol. 47, no. 4, pp. 610–617, 2009.

[7] X. Li, Y. Chen, M. V. Barnhart, X. Xu, and G. Huang, "Tailoring vibration suppression bands with hierarchical metamaterials containing local resonators," *J. Sound Vib.*, vol. 442, pp. 237–248, 2018.

[8] Z. Liu, C. T. Chan, and P. Sheng, "Analytic model of phononic crystals with local resonances," *Phys. Rev. B - Condens. Matter Mater. Phys.*, vol. 71, no. 1, pp. 1–8, 2005.

[9] X. Zhou and G. Hu, "Analytic model of elastic metamaterials with local resonances," *Phys. Rev. B - Condens. Matter Mater. Phys.*, vol. 79, no. 19, pp. 1–9, 2009.

[10] J.-L. Auriault and G. Bonnet, "Dynamique des composites élastiques périodiques," *Arch.Mech.*, vol. 37, no. January 1985, pp. 269–284, 1985.

[11] K. Pham, A. Maurel, and J. J. Marigo, "Two scale homogenization of a row of locally resonant inclusions - the case of anti-plane shear waves," *J. Mech. Phys. Solids*, vol. 106, pp. 80–94, 2017.

[12] J. Marigo and C. Comi, "Homogenization approach and Bloch-Floquet theory for band-gap prediction in 2D locally resonant metamaterials," *submitted*, 2019.

[13] G. Allaire, "Homogenization and two-scale convergence," *Siam J. Math. Anal.*, vol. 23, no. 6, pp. 1482–1518, 1992.

[14] M. Åberg and P. Gudmundson, "The usage of standard finite element codes for computation of dispersion relations in materials with periodic microstructure," *J. Acoust. Soc. Am.*, vol. 102, no. 4, pp. 2007–2013, 1997.

[15] C. Comi and L. Driemeier, "Wave propagation in cellular locally resonant metamaterials," *Lat. Am. J. Solids Struct.*, vol. 15, no. 4, pp. 1–15, 2018.

[16] C. Kittel, *Elementary solid state physics: a short course*. 1962.

[17] A. S. Phani, J. Woodhouse, and N. A. Fleck, "Wave propagation in two-dimensional periodic lattices," *J. Acoust. Soc. Am.*, vol. 119, no. 4, pp. 1995–2005, 2006.